Geoderma 2019, 353, 213–226

Pre-publication copy

https://doi.org/10.1016/j.geoderma.2019.06.032

Driving factors of soil organic carbon fractions over New South Wales, Australia

Jonathan Gray[a,*], Senani Karunaratne[b], Thomas Bishop[c], Brian Wilson[d] and Manoharan Veeragathipillai[e]

[a] NSW Office of Environment and Heritage, Parramatta, NSW 2124, Australia

[b] formerly University of Sydney, now Agriculture Victoria Research, Ellinbank, VIC 3821, Australia

[c] Sydney Institute of Agriculture, University of Sydney, NSW 2006, Australia

[d] University of New England and NSW Office of Environment and Heritage, Armidale, NSW 2351, Australia

[e] NSW Office of Environment and Heritage, Yanco, NSW 2703, Australia

[*] Corresponding author: Email: jonathan.gray@environment.nsw.gov.au

Abstract

We modelled and mapped the distribution of three principal soil organic carbon (SOC) fractions across New South Wales and gained insights into the factors controlling their distribution. Carbon fractions are important for modelling soil carbon dynamics for carbon accounting, and as a potential indicator of soil quality. We considered particulate organic carbon (POC), humic organic carbon (HOC) and resistant organic carbon (ROC), which represent fractions of increasing bio-chemical stability. A dataset of 427 NSW profiles with mid-infrared (MIR) derived carbon fractions and a set of 16 predictor variables were applied. Random Forest and multiple linear regression techniques were applied, for depth intervals to 30 cm.

The derived models and maps were of moderate strength, with validation results revealing Lin's concordance values for the 0-30 cm depth interval of 0.79 for total SOC stocks and 0.60 to 0.74 for the fraction stocks. Maps of mean stocks, and upper and lower 95% prediction intervals are presented. Absolute stocks (in Mg ha^{-1}) of each fraction have a strong linear relationship with total SOC and are controlled by similar environmental and land management factors, normally increasing in a systematic way with increasingly moist climate (considering rainfall and temperatures), increasing mafic lithology (associated with more fertile, clay rich soils) and less disturbed land uses with higher vegetation cover.

The environmental factors influencing the relative proportions of each fraction (% of total SOC) are more complex, but climate and lithology appear to be dominant, in addition to depth in profile. An SOC vulnerability index is mapped over the State, identifying areas where the stored carbon is most vulnerable to land management or environmental change. Our findings add to the understanding of factors driving the distribution of soil carbon and its fractions, which may ultimately contribute to more effective climate change mitigation programs.

Keywords: carbon fractions, digital soil mapping, controlling factors, vulnerability index

1. Introduction

The storage of organic carbon in soils is a vital element in the global carbon cycle and climate change dynamics. With an estimated global soil carbon pool of 2400 billion tonnes in the top 2 m, it represents more than three times the atmospheric pool (Stockmann et al., 2013;

Batjes, 2016; Minasny et al., 2017). Organic carbon is composed of different components, or fractions, and these behave differently in the carbon cycle, with varying stability, turnover rate and consequent residence time in the soil. Thus, for the role of soil carbon to be effectively applied in global climate change models and as an avenue for mitigating human induced global warming, it is essential to understand the behaviour of the different carbon fractions, their current levels and how they respond to changes in environmental and land management drivers.

Estimates of carbon fractions are required for initialising soil carbon cycling models, such as the RothC model (Coleman and Jenkinson 1999) which model the turnover of carbon in the soil with time. This model has been adopted in national carbon accounting schemes such as FullCAM in Australia (Richards and Evans, 2004; Baldock et al., 2013a). Erroneous estimates of soil carbon pools at the model initialisation stage can contribute to considerable errors in final model predictions (Luo et al., 2017). Therefore, estimates with quantified uncertainty of these carbon fractions throughout the landscape are required for meaningful model simulations (Karunaratne et al., 2014).

Knowledge of carbon fractions is also potentially important for assessing soil quality, to inform on agricultural and ecosystem productivity and it is believed they may be more effective than total SOC in this regard (Baldock et al., 2013a, 2018; Guimaraes et al., 2013). SOC has multiple benefits in terms of biological, chemical and physical soil properties and processes (Murphy, 2015), but effects differ between the various fractions (Baldock et al., 2013a). For example, the rapid turnover of particulate organic material means it provides more energy to soil organisms than the more resistant forms, while humic material can be more effective as a source of micronutrients to plants and in alleviating heavy metal toxicity and metal deficiency (Guimaraes et al., 2013). POC has been used instead of total SOC as a sensitive indicator of change in soil quality (Chan et al., 2002; Haynes, 2005).

Several different schemes have been developed to classify soil carbon fractions, including those reported by Six *et al*. (2001), Zimmermann *et al*. (2007) and Poeplau et al. (2018). A scheme widely used in Australia is that of Skjemstad et al. (2004), later modified by Baldock *et al*. (2013b), which recognises three main fractions: (i) particulate organic carbon (POC) fresh organic inputs, <2 mm and >50 µm; (ii) humic organic carbon (HOC) microbially altered materials associated with mineral particles, <50 µm*;* and (iii) resistant organic carbon (ROC), charcoal-like material, <2 mm. These represent fractions of increasing stability, with decomposition timescales ranging from days to potentially thousands of years (Baldock et al., 2013b; Stockmann et al., 2013; Wilson et al., 2017). They are considered to be representative of the conceptual carbon pools applied in the RothC soil carbon cycling model (Skjemstad et al., 2004).

Much research has been carried out on mapping and modelling of total SOC, including the elucidation of factors controlling its distribution and behaviour under changing land use and management, both in Australia (e.g., Viscarra Rossel et al., 2014; Hobley et al. 2015; Gray et al., 2015a) and around the world (e.g., Hengl et al., 2014; Xiong et al. 2014; Minasny et al., 2013, 2017; Angst et al. 2018; Wiesmeier et al., 2019). However, relatively little equivalent research has been undertaken relating to individual carbon fractions, although this is now being addressed. Viscarra Rossel et al. (2019) have recently completed comprehensive SOC fraction mapping and analysis over continental Australia. Regional scale mapping has been undertaken by Vasques et al. (2010), Karunaratne et al. (2014), Ahmed et al. (2017) and Keskin et al. (2019). Recent research on the influence of environmental and land management factors has also been carried out by Guimaraes et al. (2013); Page et al. (2013); Rabbi et al. (2014); Wiesmeier et al. 2014; Hobley et al. (2016); Luo et al. (2017); Orgill et

al. (2017); Wilson et al. (2017); Vos et al. 2018 and Zhang et al. (2018). The need for further research on the composition of SOC and associated changes under different environmental and management regimes was noted as key to the successful modelling of SOC dynamics by Stockmann et al. (2013).

In this project we aimed to model and map at high spatial resolution the distribution of carbon fractions across the State of New South Wales (NSW), Australia and gain insights into the factors driving this distribution. Such results may contribute to our knowledge and understanding of the long-term storage of carbon is soils and ultimately assist NSW to meet its goal of net zero emissions by 2050 (NSW Government, 2016) and contribute to climate change mitigation programs more broadly. Initial soil data were derived from the NSW Government monitoring program carried out in 2008-09 (OEH, 2009). The acquisition of carbon fraction data involved the use of a mid-infrared (MIR) spectroscopic techniques following the procedure outlined by Baldock et al. (2013a). Specific aims were to:

- map the absolute stocks (Mg ha^{-1}) of three carbon fractions (POC, HOC and ROC) at 100 m resolution across NSW
- map the relative proportions (in %) of the three fractions across the State
- assess the key environmental and land management driving factors for both absolute and relative contents of these fractions
- explore the application of a soil carbon vulnerability index across the State.

2. Methods

2.1. Overview

The study covered the entire state of NSW in eastern Australia, which covers an area of 810 000 km^2, slightly larger than France or Texas (Figure 1). A broad overview of its geography is provided in Gray et al. (2016). A dataset of soil profiles was used to develop Random Forest (RF) and multiple linear regression (MLR) models to describe the relationship of total SOC and the three SOC fractions to a range of environmental and land use variables representing key soil forming factors. Models were prepared for the 0-10, 10-30 and 0-30 cm intervals. The RF models were used to generate digital soil maps (at 100 m resolution) for each fraction at each depth interval. Variable importance plots from the RF models, in conjunction with standardised regression coefficients from the MLR models, were used to inform on the relative influence of the variables on each carbon fraction. Absolute levels and relative proportions of each carbon fraction were examined.

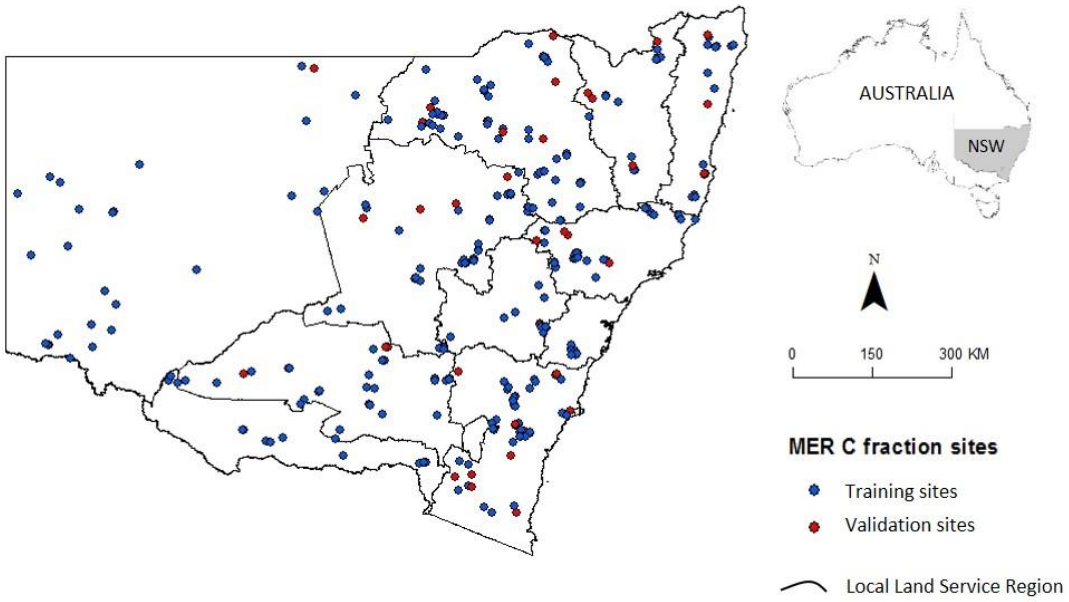

Figure 1: MER sites with carbon fraction data, NSW

(note: at this scale many points are overlapping so not all sites are evident)

2.2. The soil dataset

The carbon fraction dataset was derived from the NSW Monitoring, Evaluation and Reporting (MER) program of the NSW Government during 2008-09 (OEH, 2009, 2014). It comprised 799 profiles with total SOC, of which 427 profiles also included the three carbon fractions: HOC, POC and ROC (Figure 1). Four depth intervals down to 30 cm were included (0-5, 5-10, 10-20 and 20-30 cm). Bulk density, plus electrical conductivity and soil colour, together with extensive field and land management data were also included. The values were averaged with weighted means, based on depth, to produce values for the 0-10, 10-30 and 0-30 cm intervals.

Laboratory analysis was carried out at the Office of Environment and Heritage (OEH) Soil Health and Archive Laboratory, at Yanco, NSW. Total SOC was determined using the LECO dry combustion method (Rayment and Lyons, 2011). The fractions POC, HOC and ROC were estimated using mid-infrared (MIR) spectroscopy techniques combined with partial least squares regression (PLSR) modelling. The calibration dataset used to develop the PLSR models was derived from samples collected during the national Soil Carbon Research Program (SCaRP, Sanderman et al., 2011) and the NSW MER program. The MIR-PLSR methodology adopted followed that described by Baldock et al. (2013a&b). Validation of the MIR-PLSR derived fractions against C^{13} nuclear magnetic resonance spectroscopy (NMR) derived measurements from 80 independent external samples revealed R^2 values of 0.79, 0.96 and 0.91 for POC, HOC and ROC respectively. The Mahalanobis distance statistic was less than 3 for all validation samples, which provided further confidence in the reliability of the MIR-PLSR predictions. Further technical detail on the laboratory methods used to derive the carbon fractions in this study, including the precise equipment and software used, is presented in Wilson et al. (2017).

SOC density (kg m^{-3}) was added to the dataset by applying the bulk density values using the following simple relationship: SOC (kg m^{-3}) = SOC% x BD (Mg m^{-3}) x 10. These values

were converted into carbon stocks (Mg ha^{-1}) for each layer. Bulk density of all soil samples was calculated following both NSW and National Protocols (OEH 2009; Sanderman et al., 2011). It was based on the mass of the 2 mm sieved fraction per unit volume with correction for both soil moisture and gravel (>2 mm) content.

2.3. Selection of environmental variables

Variables were selected to effectively represent each of the key soil-forming factors of climate, parent material, relief, biota and age, as outlined below. Further detail on each variable is provided in the cited references. Data was restricted to continuous or ordinal categorical data sets; with nominal categorical data sets such as soil type being avoided. Abbreviations used to define the variables in the plots are given in brackets and italics.

2.3.1. Climate

- Mean annual rainfall (mm pa, *rainfall*) derived from 2.5-km Australia-wide climate grids from the Australian Bureau of Meteorology with resampling to a spatial resolution of 100-m. The values represent mean values obtained over the 1961–90 period, which slightly predates the period when the soil profiles were collected
- Mean annual daily maximum temperature (^{o}C, *temp_max*) – as above)
- Rainfall/max temperature ratio *(R/Tm ratio)*— the ratio of the above two covariates was derived to provide a single climatic index, used only for post modelling interpretation purposes. We classified this into three classes: (i) dry: <=20; (ii) moist: 20–50; (iii) wet: >50.

2.3.2 Parent material

- Lithology_index – refers to the lithology of the parent material, and more specifically the silica content (%), which provides a simple but meaningful quantitative estimate of the chemical composition of most parent materials. It generally has a direct relationship to quartz content and an inverse relationship with basic cation content (Gray et al., 2016). Higher silica content parent materials typically give rise to soils with more quartzose and sandier textures with lower chemical fertility. For post modelling interpretation purposes, just four lithology classes were applied: (i) mafic (e.g., basalt, <=52% silica); (ii) intermediate (e.g., diorite, 52-65% silica); (iii) siliceous lower (e.g., granodiorite, 65-75%) and (iv) siliceous upper (e.g., quartz sandstone, >75% silica).

  For model development, the description of parent material or geologic unit recorded at each site by the soil surveyor was used. For the final map preparation, lithological classes were applied manually to each geological formation as identified in the 1:250 000-scale digital geology map of the Geological Survey of NSW (undated) together with soil type data from OEH (2018) to better represent Cainozoic alluvial material, as described in Gray et al. (2016).

- Gamma radiometrics – radiometric potassium (*rad_K*), uranium (*rad_U*) and thorium (rad_Th); 90-m grids developed by and sourced from Geoscience Australia (Minty et al., 2009).
- NIR clay components – the relative proportions of kaolin, illite and smectite clays (e.g., *kaolin_propn*) derived from DSM techniques based on laboratory near infra-red (NIR)

spectroscopy (Viscarra Rossel, 2011); 90-m grids sourced through the CSIRO Data Access Portal (https://data.csiro.au/dap/search?q=TERN+Soil).

2.3.3. Relief

- Topographic wetness index (*topo_wet_index*) – a widely used index that represents potential hydrological conditions based on slope and catchment area, as derived from 30 m resolution digital elevation models (DEMs) (Gallant & Austin, 2015); sourced through the CSIRO Data Access Portal.
- Topo-slope index – an index that combines topographic position and slope gradient, representing the degree to which a site is subject to depletion (1) or accumulation (6) of water, soil particles and chemical materials. Data was derived from field data and a 100-m DEM (Gray et al., 2015b).
- Slope (*slope_pc*) – slope gradient in percent as derived from a 100-m DEM.
- Aspect index – an index to represent the amount of solar radiation received by sites, ranging from 1 for flat areas and gentle north or north-west facing slopes (high radiation in southern hemisphere) to 10 for steep south and south-east facing slopes (low radiation) (Gray et al., 2015b).

2.3.4. Biota

- Land disturbance index (*land_disturb_index*) – an index that reflects the intensity of disturbance associated with the land use (Gray et al., 2015b), where 1 denotes natural ecosystems and 6 denotes intensive cropping, based on 1:25 000-scale land-use mapping (OEH, 2017).
- Vegetation cover (*veg_frac_cover*) – total vegetation cover % (photo-synthetic and non-photo-synthetic), being average (mean) cover over the 2006-2008 period, derived from CSIRO MODIS fractional vegetation data (Guerschman and Hill, 2018). For post modelling interpretation purposes this was classified into just three vegetation cover classes: (i) <=65% mean cover, (ii) 65-85% mean cover and (iii) >85% mean cover.

2.3.5. Age

- Weathering index – an index to represent the degree of weathering of parent materials, regolith and soil, based on gamma radiometric data (Wilford, 2012); 90-m grids were sourced from Geoscience Australia. The index is considered to reflect the age of the soil.

2.4. Spatial modelling, mapping and quality assessment

All analysis was carried out using R statistical software (R Core Team, 2018). The soil dataset was apportioned 80% as training data and 20% as validation data (Figure 1) using a simple random data splitting approach with modelling by random forest (RF) decision tree models (*randomForest* package, Liaw and Wiener, 2018) and multiple linear regression (MLR). Final maps were prepared with the RF models, using 10 bootstrap samples and stacking the resulting outputs (using customised code with the abovementioned package). The 10 bootstrap iterations were considered sufficient for the purpose of this study. A natural log transformation was applied to the SOC values to achieve normality. Initial models were prepared for SOC density (kg m^{-3}), but the final maps were presented as SOC stocks (Mg ha^{-1}). Upper and lower 95% prediction interval maps were derived using results from the 10 RF iterations. Models and maps were also prepared for the relative proportions of each carbon fraction (i.e., their percentage proportion of total SOC).

The models and final maps for each depth interval were validated using the validation datasets as an independent assessment of model quality. Lin's concordance correlation coefficient (LCCC) from the *epiR* package (Stevenson, 2019) was used to measure the level of agreement of predicted values with observed values relative to the 1:1 line (Lin 1989). Root mean square error (RMSE) and mean error of validation results were also determined. These statistics, together with the confidence interval maps, provide an indication of uncertainty levels sufficient for the primary purpose of this study.

Variable importance plots from the RF models were used together with standardised regression coefficients in the MLR models (using *beta* function in *QuantPysch* package, Fletcher, 2019) to inform on the relative influence and direction of influence of each variable. Bar plots showing carbon fraction stocks for each of 36 combinations of (i) climate regime (R/*T*m_ratio), (ii) lithology class and (iii) vegetation cover class were prepared to further inform on key distribution trends. The mean stocks and 90% confidence intervals (based on 1.645 x standard deviation) are shown for each environmental combination.

The three fractions were combined into a single index called the SOC vulnerability index, designed to asess the overall stability or vulnerability of SOC in a soil. Our index follows that of Baldock et al (2018):

$$SOCVI = POC / (HOC + ROC) * 100 \quad (1)$$

This compares the fraction with a short turnover period (POC) against the fractions with longer term turnover periods (HOC and ROC). A spatial map of SOCVI at 100 m resolution was produced over the 0-30 cm interval across NSW.

3. Results

3.1. Statistical performance of maps

Validation of the final digital soil maps for total SOC and the three fractions revealed moderate performance (Table 1). LCCC values varied between 0.70 and 0.79 for total SOC stocks and between 0.52 and 0.77 for the OC fraction stocks. RMSE values generally varied between 1.2 and 8.5 Mg ha^{-1} for the fraction stocks. Map performance was better in the surface (0-10 cm) interval than the subsurface interval (10-30 cm). POC showed the greatest difference in strength between the upper and lower intervals, with LCCC values of 0.77 and 0.52 respectively.

Table 1. Map validation results

Property	Depth (cm)	N	LCCC	RMSE	Mean error
Total SOC stock	0-10	142	0.75	10.3	0.1
(Mg ha^{-1})	10-30	142	0.70	11.2	0.2
	0-30	142	0.79	17.5	1.3
POC stock	0-10	76	0.77	1.6	0.4
(Mg ha^{-1})	10-30	76	0.52	1.2	0.1
	0-30	75	0.74	2.3	0.7
HOC stock	0-10	76	0.62	3.9	0.8
(Mg ha^{-1})	10-30	76	0.68	5.8	-0.2
	0-30	76	0.69	8.5	0.8
ROC stock	0-10	76	0.62	2.0	0.3
(Mg ha^{-1})	10-30	76	0.59	3.3	-0.1
	0-30	76	0.60	4.8	0.4

The consistency of predictions of the ten bootstrap predictions over the validation points is shown by the standard deviations and standard errors from the means in Table S1 in Supplementary Information. The standard deviations and errors are low relative to the means.

3.2. Absolute stocks of SOC fractions

Final maps of carbon fraction stocks across NSW (0-30 cm interval), with lower and upper 95% prediction intervals, are shown in Figure 2. Maps for 0-10 and 10-30 intervals for each fraction are presented in Figures S1 and S2 in Supplementary Information. The maps demonstrate that all three fractions increase from west to east across NSW as conditions become more moist. HOC has the highest stocks, followed by ROC then POC. HOC is highest in northern and central NSW coastal areas and in highland areas characterised by mafic lithology (high fertility soils) (>35 Mg ha^{-1}). Moderately high stocks (25-30 Mg ha^{-1}) are also evident in the cereal belt of central west slopes and plains. Lowest levels (7.5-12 Mg ha^{-1}) of HOC occur in the far north west of State, where the climate is hottest and driest.

ROC and POC show similar declines from east to west, albeit at lower absolute levels (ROC: 25 to 7 Mg ha^{-1}; POC: 12 to 3 Mg ha^{-1}). In contrast to HOC, they reveal relatively low levels in the cereal belt of western slopes and plains, particularly POC (<7 Mg ha^{-1}).

The stocks of total SOC and each fraction in 36 different climate—parent material—vegetation cover classes are presented in Figures 3 and 4. These plots all reveal broadly consistent trends with these environmental variables (as shown by the trend line). They demonstrate that the combined influence of these variables controls the final stock levels of total SOC and each fraction. They clearly reveal increasing stocks with increasingly moist climate (considering combined rainfall and temperature), increasingly mafic parent material (more fertile clay rich soils) and increasing vegetation cover.

These results are broadly supported by the variable importance plots from the random forest models (Figures 5 and Figure S3 in Supplementary Information), together with standardised regression coefficients from the MLR models (see Tables S2 and S3 in Supplementary Information), which reveal the main factors influencing the stocks of total SOC and each fraction. The direction of influence is indicated by the positive and negative signs. The mass of each fraction tends to increase with increasing rainfall, mafic lithology and vegetation cover together with lower temperatures and lower land use disturbance. There are, however, a few apparent exceptions to these trends. HOC, and to a lesser extent ROC, appear to increase with increasing temperatures. Lithology appears to have a low influence on POC, particularly in the 0-10 cm depth interval. The degree of influence suggested for different variables differs somewhat between the variable importance plots (from RF models) and the standardised regression coefficients (from MLR models).

Topography is revealed to have relatively minor influence at the scale of this study with no clear trends evident. All three fractions display a slight increase with higher weathering index, the same as for total carbon. Trends with clay proportions are somewhat ambiguous. In relation to radiometric variables, total SOC, POC and ROC have a positive relationship with radiometric K and U, but a negative relationship with radiometric Th. For HOC, there appears to be a weak positive relationship with all three radiometric elements.

The concentration and mass (in kgm^{-3}) of each fraction typically declines with depth, as shown by the mean values presented in Table 2. The influence of variables also differs slightly according to depth, as can be observed from variable importance plots for 0-10 and 10-30 cm intervals presented in Figure S3, Supplementary Material. For each fraction,

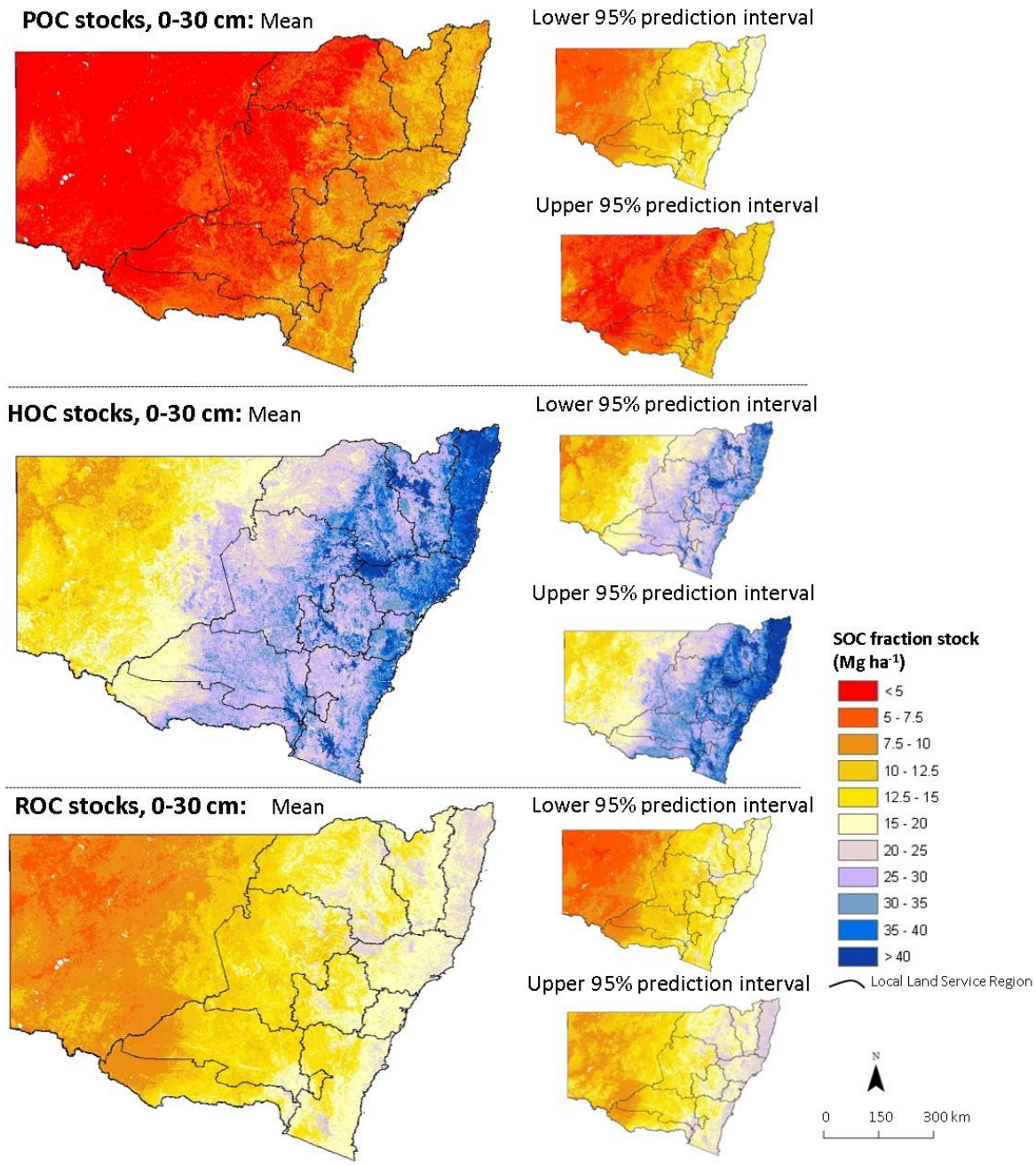

Figure 2: SOC carbon fraction stocks over NSW, mean and upper and lower 95% prediction intervals, 0-30 cm (Mg ha^{-1})

rainfall, vegetation cover and land use are highly influential in the upper interval but less influential in the lower interval. Lithology displays the reverse trend. Temperature is more influential in upper depths for total SOC and POC but appears to be the reverse for HOC and unchanged for ROC. Topographic variables tend not to vary significantly in their influence over the two depths.

The similarity in controlling trends for each carbon fraction and total SOC is expected given the positive linear relationship between them, as shown by Figure 6. For the 0-30 cm interval, the R^2 values range from a low of 0.38 for POC to a high of 0.67 for HOC.

Table 2: Absolute mass and relative proportions of each fraction at different depth intervals across NSW

	Absolute mass (kgm^{-3})			Relative proportion (%)		
	0-10 cm	10-30 cm	0-30 cm	0-10 cm	10-30 cm	0-30 cm
POC	3.33	1.05	1.98	16.8	9.7	14.0
HOC	9.84	6.64	7.97	53.9	58.0	55.6
ROC	5.23	3.59	4.24	29.3	32.3	30.4

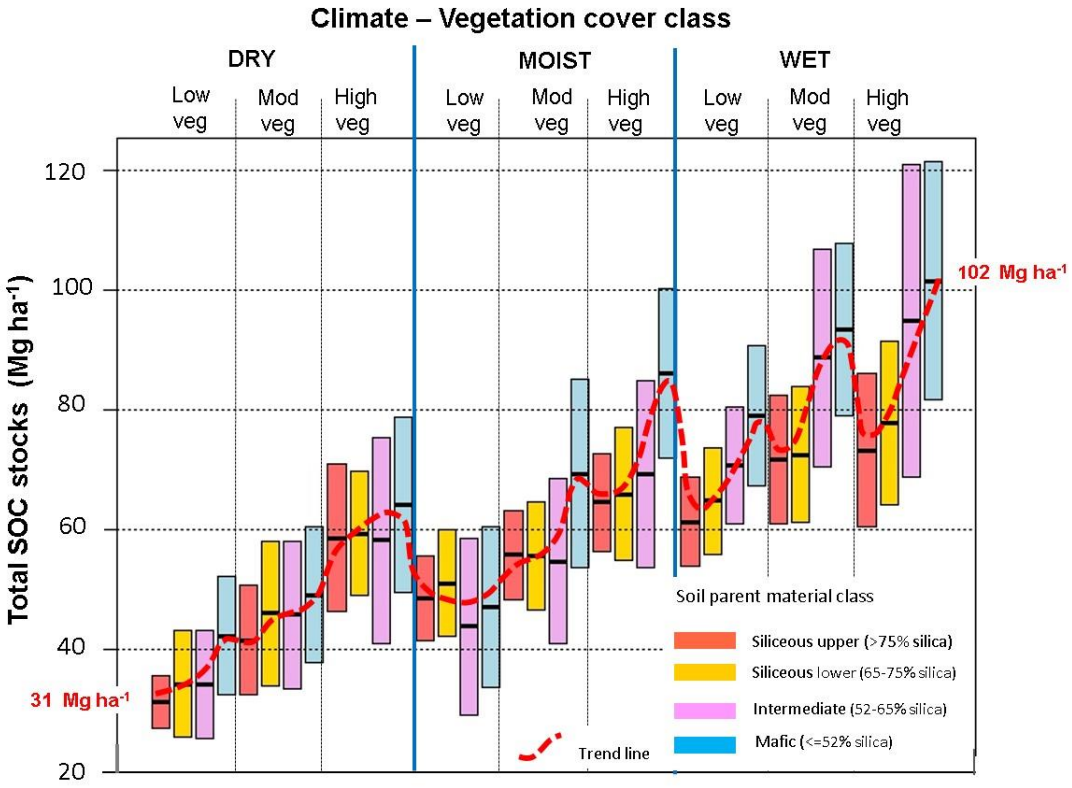

Figure 3: Variation in stocks of total SOC with different climate-parent material-vegetation cover classes, with 90% spread of predictions, 0-30 cm

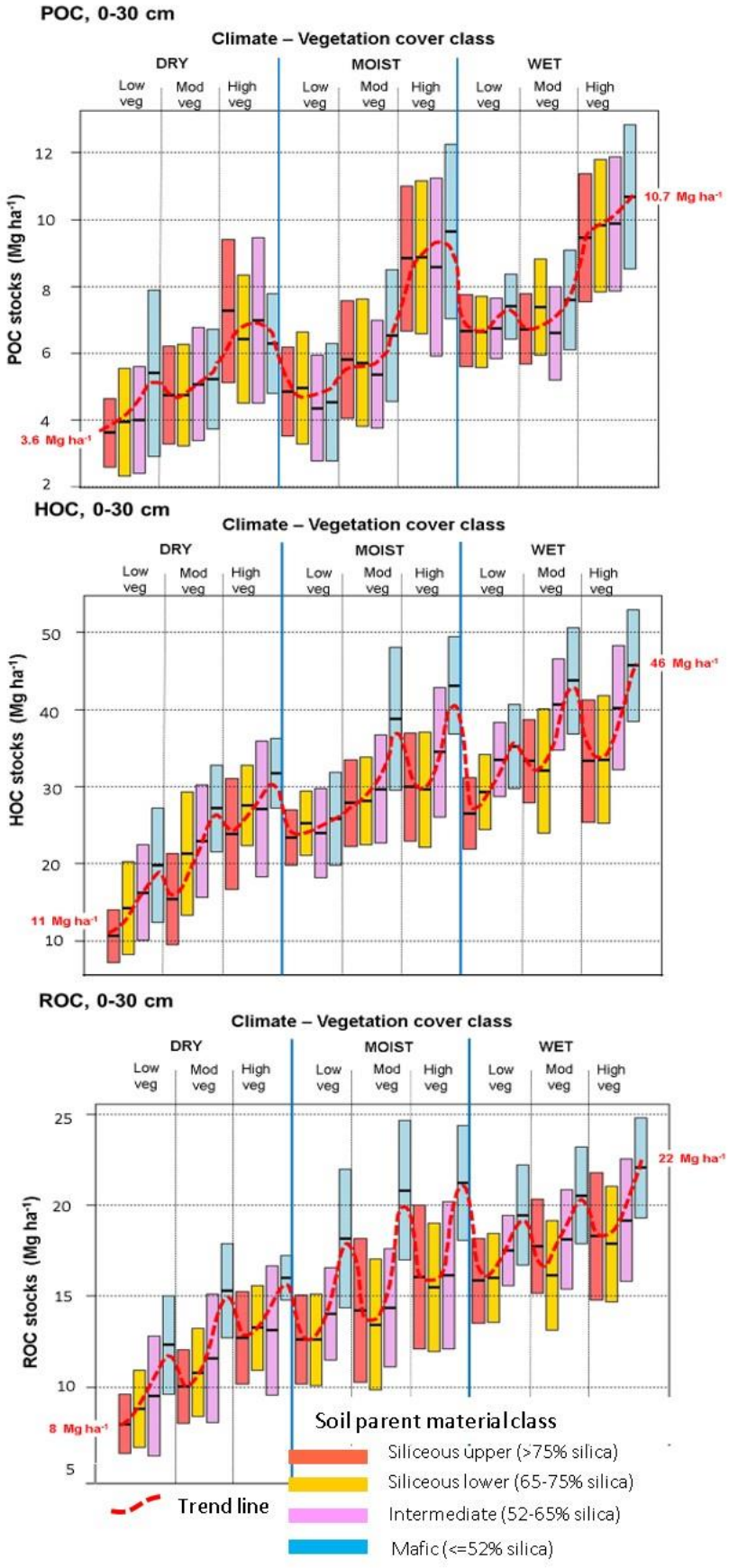

Figure 4: Variation in stocks of carbon fractions with different climate-parent material-vegetation cover classes, with 90% spread of predictions, 0-30 cm

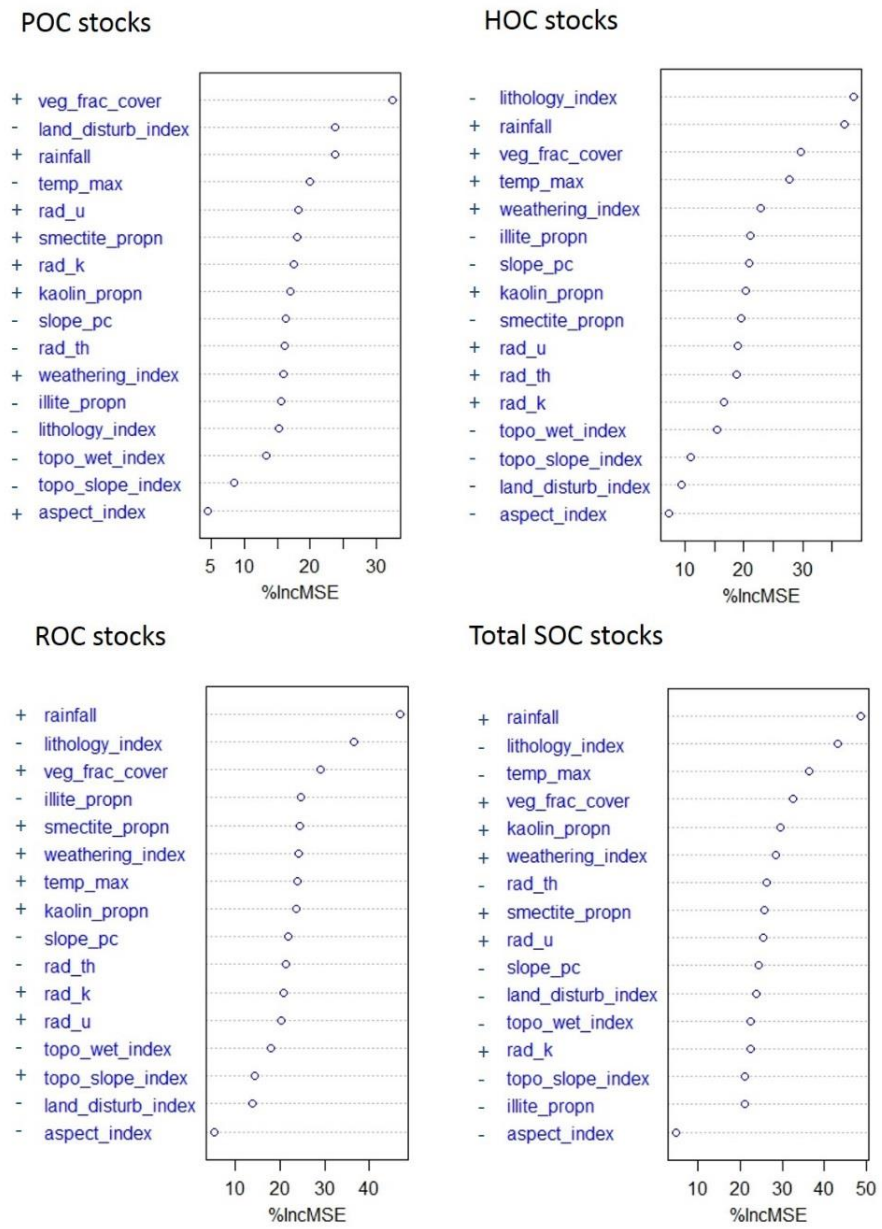

Figure 5: Variable importance plots for absolute stocks of the three carbon fractions, 0-30 cm (+ or – sign gives direction of influence)

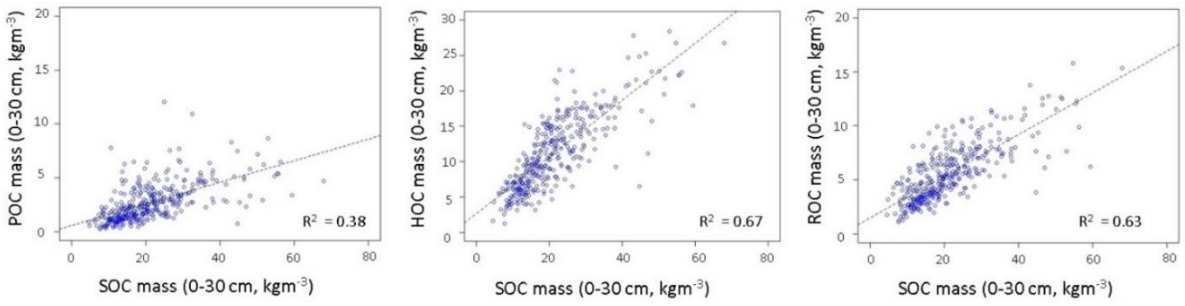

Figure 6: Relationship of the three carbon fractions with total SOC, 0-30 cm (all observed values)

3.3. Relative proportions of SOC fractions

From Table 2 it is evident that HOC has the highest proportions at all depth intervals (mean for 0-30 cm interval of 55.6%), followed by ROC then POC (respective means of 30.4% and 14.0% for 0-30 cm). POC reduces in relative proportion from the upper (0-10 cm) interval to the lower (10-30 cm) interval from 16.8 to 9.7%, while both HOC and ROC display a slight increase in relative proportions.

The proportions of each of the three carbon fractions for the 0-30 cm interval, as derived by using ratios of the absolute stocks for each pixel in the maps of Figure 2, are shown in the maps of Figure 7. It is difficult to draw clear patterns of distribution across the state from these maps, suggesting patterns are complex and controlled by a combination of factors.

The proportion of POC is generally lowest in the western slopes and plains, in a broad belt extending from the north to the south of the State (<12%). This region is typified by grain cropping, warm temperatures with low-moderate rainfall and moderately fertile soils. It is highest in the Tableland regions extending from north to south in the east, which are generally associated with cool moist conditions. HOC generally displays the reverse trends, being highest in the central western and south western slopes and plains of NSW (60-75%). The proportion of ROC is highest in the northern slopes and plains and in the west of the State (generally 30-40%) characterised by warm dry conditions. The lowest proportions of ROC occur in the central western slopes and plains (20-25%).

Figure 8 presents the trends in proportions of each fraction over the 36 climate—parent material—vegetation cover classes as applied for absolute stocks in Figures 3 and 4. Although some anomalies are apparent, broad trends are revealed for each fraction. With respect to moisture regime (considering combined rainfall and temperatures) the proportion of HOC tends to increase with moister conditions, the proportion of ROC tends to increase with drier conditions, while POC proportions appears unresponsive. With respect to parent material (influencing soil type), the proportion of POC and ROC both display an increase with more siliceous parent materials (less fertile soils) while HOC displays the reverse trend. With respect to vegetation cover, ROC displays an increase with lower cover, while POC and HOC reveal no consistent trends.

An examination of the distribution patterns of relative proportions of the three fractions relative to vegetation cover and land use reveal complex relationships with no clear patterns. Apparent anomalies in the trends for HOC and ROC revealed in Figure 8 coincide with the cereal cropping belt of the central western slopes and plains, which also suggests complex relationships of the SOC fractions with land use. Higher proportions of ROC in lower parts of the landscape are evident from the fine scale distribution patterns.

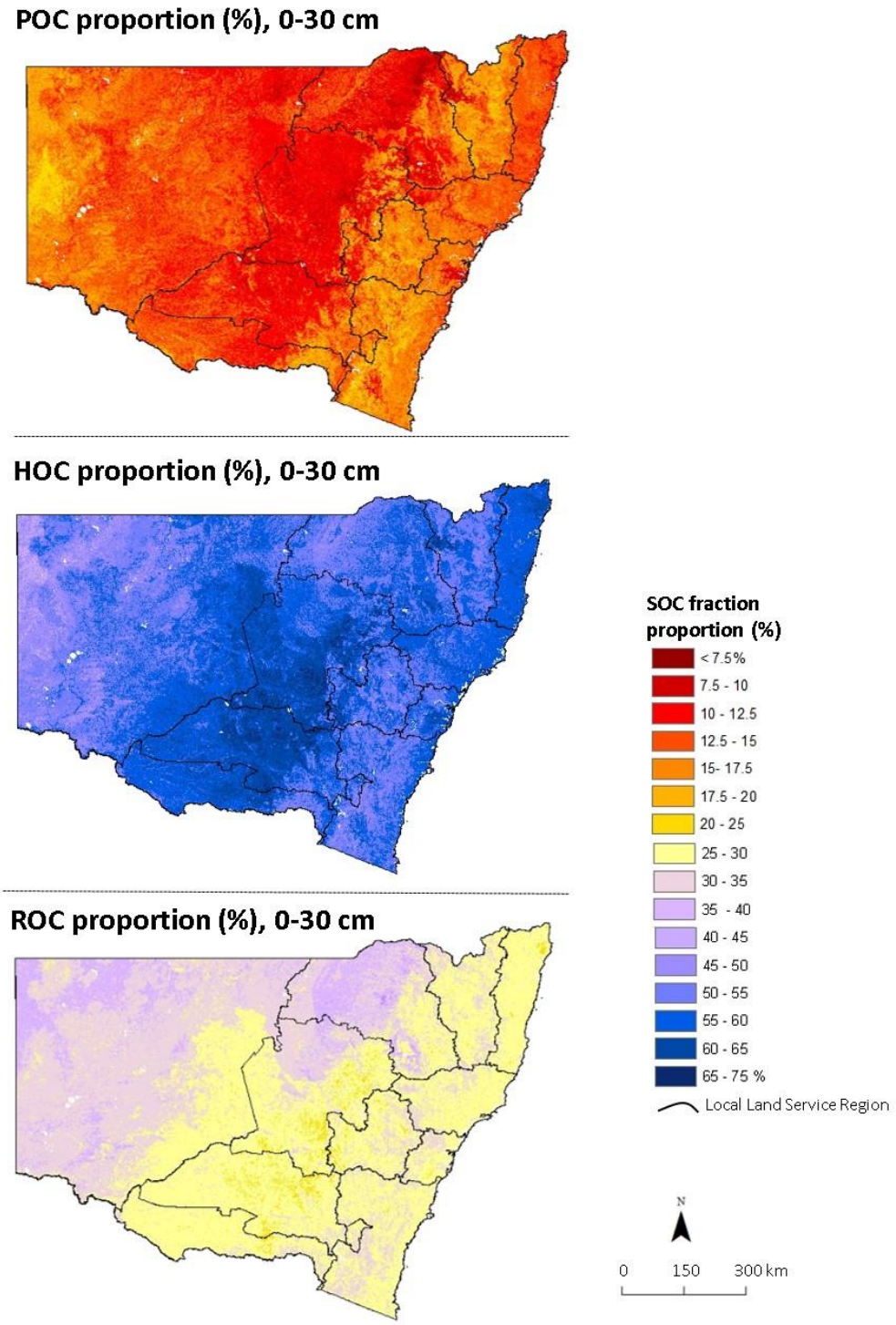

Figure 7: Proportions of carbon fraction relative to total SOC stocks over NSW, 0-30 cm (%)

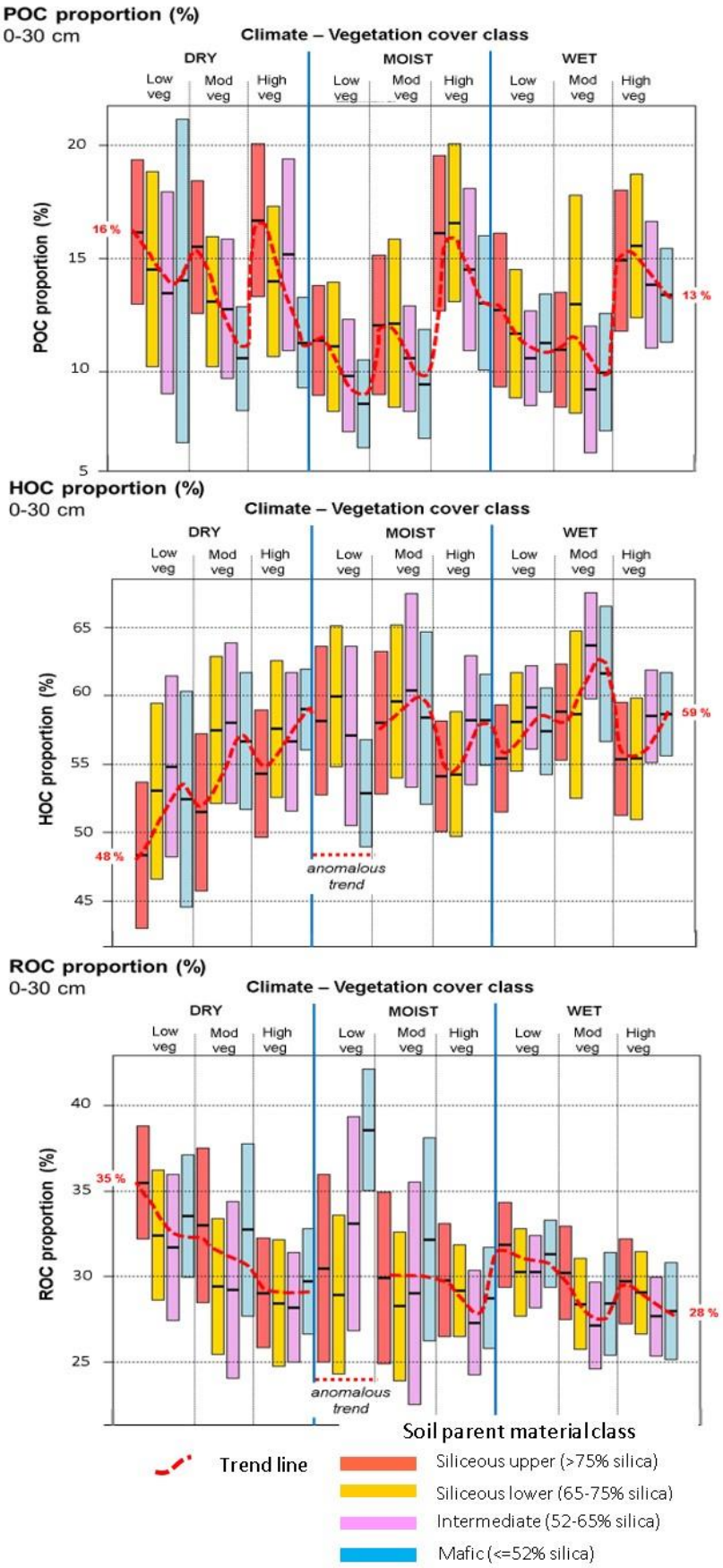

Figure 8: Variation in relative proportions of carbon fractions with different climate-parent material-vegetation cover classes, with 90% spread of predictions, 0-30 cm (%)

3.4. SOC vulnerability index across NSW

The map of the SOC vulnerability index for the 0-30 cm interval across NSW is presented in Figure 9.

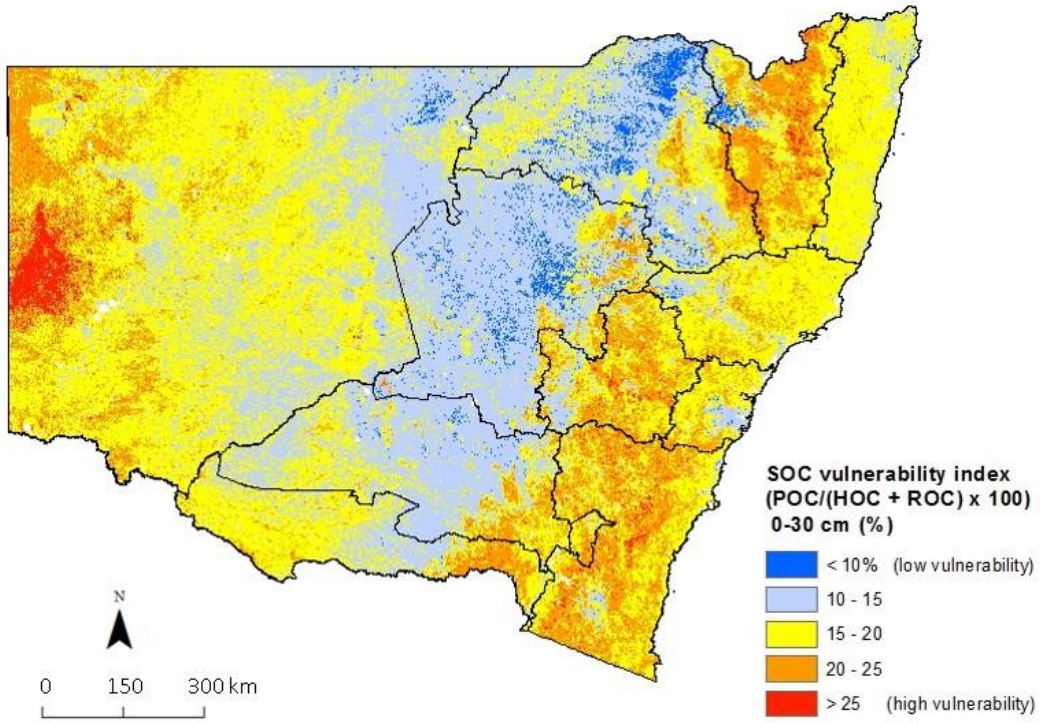

Figure 9: SOC vulnerability index across NSW, 0-30 cm

The map reveals the lowest vulnerability indices (i.e., stable carbon least susceptible to land management change) in a central belt extending from north to south across NSW, characterised by mixed grazing and cropping in a dry-moderate rainfall zone. The highest indices (i.e., the least stable carbon, most susceptible to land management change) occur in the eastern tablelands typified by cool, moist grazing and forest land and also in the dry grazing lands in the far west of the State.

4. Discussion

4.1. Model and map performance

The total SOC mass map had moderate to high validation performance, with LCCC values up to 0.79 but the individual fractions were typically of only moderate performance, with LCCC values generally in the range 0.60 to 0.70. The maps were typically more reliable in the upper depth soils, becoming less reliable in the deeper soils. The total SOC map performance compares well with other SOC modelling in Australia and worldwide. Results presented by Minasny et al. (2013) for projects for areas greater than 500 km^2 reveal R^2 values between 0.2 and 0.6, which may equate to LCCC values of approximately 0.5 to 0.8.

Few studies have attempted to map the distribution of carbon fractions, so there is little to compare the relative performance of our models and maps with. Our maps appear broadly consistent in stock predictions and trends with the recently released Australia-wide maps of Viscarra Rossel et al. (2019). Those maps achieved validation LCCC values of between 0.53 to 0.78 depending on the fraction and validation approach. Karunaratne et al. (2014) achieved similar validation values in their mapping of SOC fraction densities to 0.3 m depth in a regional catchment of northern NSW. Keskin et al. (2019) achieved LCCC values up to 0.83 for recalcitrant carbon, but only 0.47 for labile carbon over Florida, USA. The two latter studies revealed the lowest model performance for the POC/labile fractions, which is similarly suggested in our study by the low LCCC value of 0.49 for the 10-30 cm interval for POC.

Although of variable strength, the models and maps produced in this study could be applied in conjunction with the recently released Australia-wide maps of Viscarra Rossel et al. (2019) to provide useful approximations of SOC fractions across NSW. They provide necessary input data for carbon dynamic models such as RothC, and for use in carbon accounting schemes such as FullCAM in Australia (Richards and Evans, 2004). They allow these carbon models to be initialised without prior land use history across the landscape or the need to run them to an equilibrium state. The models and maps are of sufficient strength to facilitate interpretation of factors driving the distribution and relative abundances of the carbon fractions.

4.2. Factors influencing carbon fraction levels

It has been demonstrated that in terms of absolute stocks of each of the three fractions across NSW, the controlling environmental and land management factors are generally the same as those controlling total soil organic carbon. Thus, the higher the total SOC stocks, the higher are the stocks of each of the component carbon fractions. This is supported by the moderately strong positive linear relationships with total SOC, at least for HOC and ROC. A strong linear relationship between total SOC and the component fractions has been demonstrated by Baldock et al. (2013b), Orgill et al. (2017) and Yu et al. (2017), however, some workers have reported that the relationship is not always strong (Janik et al., 2007), as we also observed for POC (R^2 only 0.38).

The stocks of total SOC and the component fractions are shown to increase in a systematic way with increasingly moist climate (combining rainfall and temperatures), increasing mafic lithology (associated with more fertile, clay rich soils) and less disturbed land uses with higher vegetation cover. The plots of Figures 3 and 4 demonstrate that it is the combination of these factors that controls observed stock levels, similar to the plots for total SOC over all eastern Australia presented in Gray et al. (2015a). These trends for total SOC have been broadly supported by many workers throughout the world, either in part of combination, with recent examples including (Badgery et al., 2013; Minasny et al., 2013; Viscarra Rossel et al., 2014; Xiong et al., 2014; Angst et al., 2018; Wiesmeier et al., 2019).

The environmental and land management factors influencing the relative proportions of each fraction (i.e., percentage of total SOC) are more complex and deserve further research. Again, our results show it is the interplay of the combined factors that controls their relative proportions at any given location (Figure 8). The proportion of ROC appears to typically increase with drier conditions (considering combined rainfall and temperature) and lower vegetation cover while POC and HOC show no clear trends with these variables. The

proportions of POC and ROC typically appear to increase with more siliceous parent materials (less fertile soils), while HOC displays the reverse trend.

Compared to total SOC, relatively little work has been reported in the literature on the driving factors for carbon fractions, particularly for their relative proportions. Often the influencing factors are reported but not the direction of influence or any quantitative relationships. Viscarra Rossel et al. (2019) report that controlling factors for SOC fractions and their relative proportions (indicated by vulnerability index) are scale dependant and variable across regions. They suggest that the driving factors at a regional scale may differ between regions and at the continental scale.

Supporting our findings of the strong influence of climate in controlling SOC fraction levels were the studies of Karhu et al. (2010), Hobley et al. (2016), Wilson et al. (2017), Orgill et al. (2017), Zhang et al. (2018), Keskin et al. (2019) and Viscarra Rossel et al. (2019), at least at broader regional scales. Our results show rising stocks of each fraction with increasing moisture (combining rainfall and temperatures). However, they show HOC and ROC both increase with rising temperatures rather than decrease as might be expected due to the drier conditions. When considered alone, higher temperatures give rise to higher biomass production but also higher mineralisation, providing moisture levels are sufficient (Sanderman et al., 2010, Xu and Qi, 2001; Stockmann et al., 2013). The more stable HOC and ROC appear to be less subject to mineralisation and decay from rising temperatures. The greater likelihood of fire and the preferential retention of soil pyrogenic material (i.e. ROC) in drier rather than wetter regions were noted by Hobley et al. (2016).

Land management and biotic factors are frequently reported as key drivers of SOC fraction stocks. This is supported by our findings for absolute stocks of each fraction, but only marginally for their relative proportions. Page et al. (2013) demonstrate the greater loss of all fractions, including ROC, under more intensive cultivation practices, e.g., conventional versus no-tillage. The labile POC is widely reported as the most susceptible to land use and management (Janzen et al., 1992; Karunaratne et al., 2014; Yu et al., 2017; Zhang et al., 2018). Wilson et al. (2017) found HOC increasing under wetter conditions under low intensity land uses but not under high intensity agricultural land uses. However, Hobley et al. (2016) found no significant influence from land use and management in driving the relative proportions of each fraction, as also suggested by Orgill et al. (2017) with the exception of POC. Wiesmeier et al. (2014) found high proportions (90%) of intermediate and passive fractions in crop and grassland soils but lower proportions (40%) in forest soils, suggesting the greater vulnerability to potential carbon loss in forest soils.

Parent material is not frequently highlighted as a key controlling factor of SOC fractions in the published literature, in contrast to our results here that suggest it does have a strong influence. However, Orgill et al. (2017) demonstrated that basalt (mafic lithology) derived soil had significantly greater stock of total SOC, ROC and HOC to 30 cm depth compared with all other lithologies. The key role of soil type, including clay type and mineralogy, in protecting ROC is reported by Karunaratne et al. (2014). A higher proportion of ROC was reported by Hobley et al. (2016) in light textured soils at depth, a finding broadly supported by our results.

Topography is widely reported to be an important driver of total SOC only at local scales and not at province-wide scales (Minasny et al., 2013; Gray et al., 2015a; Hobley et al., 2015, Wiesmeier et al., 2019). This accords with our results here for carbon fractions, and also reported by Keskin et al (2019) in Florida. However, a positive relationship of ROC proportion with low lying points in the landscape in this study is apparent. A possible explanation for this is the erosion and deposition of charcoal like material from upper to

lower points in the landscape, a clear phenomenon reported by Abney et al. (2017) in mountainous terrain of Nevada, USA.

Depth has been shown to strongly influence carbon fraction levels, in terms of both absolute mass (in kgm^{-3}) and relative proportions (in %). As demonstrated in Table 2, absolute mass declines for each fraction from the upper to the lower depth interval, which is a well-established trend for total SOC. A decline in the relative proportion of POC with depth, together with a slight increase in the relative proportion of HOC and ROC with depth is apparent from our results. Similar trends were reported by Hobley et al. (2016), however they found no clear change with depth for ROC. They attribute the decline in POC with depth to the lesser root intensity and litter input, and the HOC increase to the downwards percolation of dissolved organic carbon and an increased availability of mineral surfaces for sorption and aggregation due to the lower POC content.

4.3. SOC vulnerability index

An SOC vulnerability index (SOCVI) has been mapped over NSW (Figure 9). The index, as promoted by Baldock et al. (2018), builds on the concepts and related indices of others (Blair et al 1995; Haynes, 2005). The index has also recently been mapped over continental Australia by Viscarra Rossel et al. (2019). Our map over NSW reveals cool, moist grazing and forest lands of NSW, as being areas where the stored soil carbon is more vulnerable to change in land use, land management or in other environmental factors, supporting the recent results of Viscarra Rossel et al. (2019). The areas of high vulnerability revealed by our map in the dry west of the State deserves more examination and were not revealed in the Australia wide maps. This and other similar indices provide an additional means of exploring the fractional composition of soil carbon across regions and of guiding strategies to protect carbon stored in the soils of NSW. In addition to carbon sequestration issues, such indices have applications as indicators of soil management practices and soil quality (Haynes, 2005; Guimaraes et al., 2013; Yu et al., 2017; Zhang et al., 2018; van Wesemael et al. 2019).

4.4. Sources of uncertainty

Reliability of the results are suggested by the validation statistics presented in Table 1 and by the upper and lower 95% prediction intervals maps of Figure 2. Reliable estimates of uncertainty are required, particularly where results are being applied in carbon accounting and financial carbon trading schemes (Mishra et al., 2010, Karunaratne et al., 2014, Malone et al., 2017). There are several issues that contribute to uncertainty in this analysis.

There are uncertainties associated with the MIR derived carbon fraction values (Somarathna et al., 2018), which will propagate through to final estimates of error. All the estimates are reliant on the representativeness of the initial calibration dataset, which for this dataset was biased towards agricultural soils, with less representation from native ecosystem soils. The Australian and NSW MIR estimates are reported to have diminishing reliability at higher SOC concentrations, above approximately 5%, due to a lack of high carbon samples in the calibration model (Wilson et al., 2017). The interpretation of spectral signatures in native ecosystems may differ from that in agricultural systems (Wilson et al., 2017). Some key trends in the distribution of individual SOC fractions and their controlling factors may be partially distorted or masked due to reliance on this imperfect calibration dataset. Differences between results from MIR and LECO derived carbon stocks have been reported by others. For example, Page et al. (2013) reported MIR total SOC under-estimated loss by 27–30% compared with LECO total SOC. They report errors in the calibration models of 7-21%.

Despite the uncertainties of MIR-PLSR derived data, it has been concluded that these are lower than the uncertainties originating from the spatial prediction process within digital soil mapping (Brodský et al., 2013; Karunaratne et al., 2014). These other uncertainties include errors in the base environmental variable grids, shortcomings in modelling techniques, inherently poor relationships between the target and environmental variables, and ineffective validation techniques (McBratney et al., 2003, Brus et al., 2011; Nelson et al., 2011; Bishop et al., 2015; Robinson et al., 2015).

Another source of uncertainty relates to the ROC fraction, chiefly comprised of char-like material, and its dependence on fire history. Such history was not included in the modelling process but is likely to be a significant controlling factor (Abney et al., 2017). The influence of erosion in redistributing this and other fractions is also a potentially key controlling factor that needs to be recognised in the modelling processes (Abney et al., 2017; Chappell et al., 2016).

5. Conclusion

Digital soil models and maps presenting the distribution of the three carbon fractions across NSW at 100 m resolution have been produced. The results have provided insights into the environmental factors driving the distribution of soil carbon fractions, in terms of both absolute stocks of each fraction and their relative proportions. Absolute stocks of each fraction have a strong linear relationship with total SOC and are controlled by similar environmental and land management factors. It is the combined influence of these factors that determines final stock levels, which normally increase with increasingly moist climate (considering both rainfall and temperatures), increasing mafic lithology (more fertile, clay rich soils) and less disturbed land uses with higher vegetation cover. In terms of relative proportions, the driving factors are more complex, but depth, climate and parent material lithology appear to be dominant. Further investigation is required to explore and clarify these important relationships.

Such knowledge and understanding on these driving factors may facilitate the development of strategies to enhance stocks of soil organic carbon and its component fractions. It will allow better identification of options and locations to promote levels of the more resistant fractions, which contribute the most to long term soil carbon storage. The results provide data to enhance modelling of soil carbon dynamics, such as initialising data within the RothC program, and thereby improve carbon accounting systems such as FullCAM in Australia. Ultimately, such knowledge on soil carbon fractions may contribute to more effective climate change mitigation programs, both locally over NSW and more globally.

Acknowledgments

The authors wish to acknowledge their respective employers at the time of preparing this paper, namely the NSW Office of Environment and Heritage, the University of Sydney and the University of New England. No external grants were received for the project.

References

Abney, R.B., Sanderman, J., Johnson, D., Fogel, M.L., Berhe, AA., 2017. Post-wildfire Erosion in Mountainous Terrain Leads to Rapid and Major Redistribution of Soil Organic Carbon. Frontiers in Earth Science, vol 5, Article 99.

Ahmed, Z.U., Woodbury, P.B., Sanderman, J., et al., 2017. Assessing soil carbon vulnerability in the Western USA by geospatial modeling of pyrogenic and particulate carbon stocks. Journal of Geophysical Research-Biogeosciences 122, 354-369.

Angst, G., Messinger, J., Greiner, M., Häusler, W., Hertel, D., Kirfel, K., Kögel-Knabner, I., et al., 2018. Soil organic carbon stocks in topsoil and subsoil controlled by parent material, carbon input in the rhizosphere, and microbial-derived compounds. Soil Biology and Biochemistry 122, 19-30.

Badgery, W.B, Simmons, A.T., Murphy, B.W., Rawson, A., Andersson, K.O. Lonergan, V.E., Van de Ven, R., 2013. Relationship between environmental and land-use variables on soil carbon levels at the regional scale in central New South Wales, Australia. Soil Research 51, 645-656.

Baldock, J.A., Beare, M.H., Curtin, D., Hawke, B., 2018. Stocks, composition and vulnerability to loss of soil organic carbon predicted using mid-infrared spectroscopy. Soil Research 56, 468-480.

Baldock, J.A., Hawke, B., Sanderman, J., Macdonald, L.M., 2013a. Predicting contents of carbon and its component fractions in Australian soils from diffuse reflectance mid-infrared spectra. Soil Research 51, 577–595.

Baldock, J.A., Sanderman, J., Macdonald, L.M., Puccini, A., Hawke, B., Szarvas, S., McGowan, J., 2013b. Quantifying the allocation of soil organic carbon to biologically significant fractions. Soil Research 51, 561–576

Batjes, N.H. 2016. Harmonized soil property values for broad-scale modelling (WISE30sec) with estimates of global soil carbon stocks. Geoderma 269, 61–68

Bishop, T.F.A., Horta, A., Karunaratne, S.B., 2015. Validation of digital soil maps at different spatial supports. Geoderma 241-242, 238-249.

Blair, G.J., Lefroy, R.D., Lisle, L., 1995. Soil carbon fractions based on their degree of oxidation, and the development of a carbon management index for agricultural systems. Australian Journal Agricultural Research 46, 1459–1466.

Brodský, L., Vašát, R., Klement, A., Zádorová, T., Jakšík, O., 2013. Uncertainty propagation in VNIR reflectance spectroscopy soil organic carbon mapping. Geoderma 199, 54–63

Brus, D.J., Kempen, B., Heuvelink, G.B.M., 2011. Sampling for validation of digital soil maps. European Journal of Soil Science 62, 394–407.

Chappell, A., Baldock, J.A., Sanderman, J., 2016. The global significance of omitting soil erosion from soil organic carbon cycling schemes. Nature Climate Change 6, 187–191. https://www.nature.com/articles/nclimate2829

Chan, K.Y., Heenan, D.P., Oates, A., 2002. Soil carbon fractions and relationship to soil quality under different tillage and stubble management. Soil and Tillage Research 63, 133–139. doi:10.1016/S0167-1987(01)00239-2

Coleman, K., Jenkinson, D.S., 1999. ROTHC-26.3. A model for the turnover of carbon in soil. Model Description and Windows User's Guide. Rothamsted Research, Harpenden, Hertfordshire, UK.

Fletcher T.D., 2019. Package 'QuantPsyc' Quantitative Psychology Tool. CRAN Repository, https://cran.r-project.org/web/packages/QuantPsyc/QuantPsyc.pdf

Gallant, J.C., Austin, J.M., 2015. Derivation of terrain covariates for digital soil mapping in Australia. Soil Research 53, 895–90.

Geological Survey of NSW, undated. 1:250 000 scale geology map of NSW. https://www.resourcesandgeoscience.nsw.gov.au/miners-and-explorers/geoscience-information/products-and-data/maps (accessed 4 March.2019).

Gray, J.M., Bishop, T.F.A., Wilford, J.R., 2016. Lithology and soil relationships for soil modelling and mapping. Catena 147, 429–440. Doi:org/10.1016/j.catena2016.07.045

Gray, J.M., Bishop, T.F.A., Wilson, B.R., 2015a. Factors controlling soil organic carbon stocks with depth in eastern Australia. Soil Science Society of America Journal 79, 1741-1751.

Gray, J.M., Bishop, T.F.A., Yang, X., 2015b. Pragmatic models for the prediction and digital mapping of soil properties in eastern Australia. Soil Research 53, 24-42.

Guerschman, J.P., Hill, M.J., 2018, Calibration and validation of the Australian fractional cover product for MODIS collection 6, Remote Sensing Letters, 9:7, 696-705. doi: 10.1080/2150704X.2018.1465611, Data at: http://www-data.wron.csiro.au/remotesensing/MODIS/products/Guerschman_etal_RSE2009/v310/australia/monthly/cover/.

Guimaraes, D.V., Silva Gonzaga, M., da Silva O., da Silva, T., da Silva Dias, N., Silva Matias, M., 2013. Soil organic matter pools and carbon fractions in soil under different land uses. Soil & Tillage Research 126, 177–182.

Haynes, R.J., 2005. Labile organic matter fractions as central components of the quality of agricultural soils: An overview. Advances in Agronomy 85, 221–268. doi:10.1016/S0065-2113(04)85005-3

Hengl, T., de Jesus, J.M., MacMillan, R.A., Batjes, N.H., Heuvelink, G.B.M., et al., 2014. SoilGrids1km — Global Soil Information Based on Automated Mapping. PLoS ONE 9(8): e105992. doi:10.1371/journal.pone.0105992

Hobley, E.U., Baldock, J., Wilson, B., 2016. Environmental and human influences on organic carbon fractions down the soil profile. Agriculture, Ecosystems and Environment 223, 152–166

Hobley, E., Wilson, B.R., Wilkie, A., Gray, J.M., Koen, T., 2015. The drivers of soil organic carbon storage and depth distribution in Eastern Australia. Plant and Soil 390:111-127.

Janik, L.J., Skjemstad, J.O., Shepherd, K.D., Spouncer, L.R., 2007. The prediction of soil carbon fractions using mid-infrared-partial least square analysis. Australian Journal of Soil Research, 45, 73-81.

Janzen, H., Campbell, C., Brandt, S.A., Lafond, G., Townley-Smith, L., 1992. Light-fraction organic matter in soils from long-term crop rotations. Soil Science Society of America Journal 56, 1799–1806.

Karhu, K., Fritze, H., Hamalainen, K., Vanhala, P., Jungner, H., Oinonen, M., Sonninen, E., Tuomi, M., Spetz, P., Kitunen, V., Liski, J 2010. Temperature sensitivity of soil carbon fractions in boreal forest soil. Ecology, 91(2), 370–376

Karunaratne, S.B., Bishop, T.F.A., Baldock, J.A., Odeh, I.O.A., 2014. Catchment scale mapping of measurable soil organic carbon fractions. Geoderma 219–220, 14–23

Keskin, H., Grunwald, S., Harris, W.G., 2019. Digital mapping of soil carbon fractions with machine learning. Geoderma 339, 40–58.

Liaw A., Wiener, M.,2018. Package ‘randomForest’ Breiman and Cutler's Random Forests for Classification and Regression. CRAN Repository, https://cran.r-project.org/web/packages/randomForest/randomForest.pdf

Lin, L.I., 1989. A concordance correlation coefficient to evaluate reproducibility. Biometrics, 45:255-268.

Luo, Z., Feng, W., Luo, Y., Baldock, J., Wang, E., 2017. Soil organic carbon dynamics jointly controlled by climate, carbon inputs, soil properties and soil carbon fractions. Global Change Biology 23, 4430-4439.

Malone, B.P., Styc, Q., Minasny, B., McBratney, A.B., 2017. Digital soil mapping of soil carbon at the farm scale: A spatial downscaling approach in consideration of measured and uncertain data. Geoderma 290, 91–99.

McBratney, A.B., Mendonca Santos, M.L., Minasny, B., 2003. On digital soil mapping. Geoderma 117:3-52.

Minasny, B, McBratney, A.B., Malone, B., Wheeler, I., 2013. Digital mapping of soil carbon. Advances in Agronomy, Volume 118, Chapter 1.

Minasny, B., Malone, B.P., McBratney, A.B., Angers, D.A., Arrouays, D., 2017. Soil carbon 4 per mille. Geoderma 292, 59–86.

Minty, B., Franklin, R., Milligan, P., Richardson, M., Wilford, J., 2009. The radiometric map of Australia. Exploration Geophysics 40, 325-333.

Mishra, U., Lai, R., Liu, D., Van Meirvenne, M., 2010. Predicting the spatial variation of the soil organic carbon pool at a regional scale. Soil Science Society of America Journal 74, 906–914.

Murphy, B.W., 2015. Impact of soil organic matter on soil properties—a review with emphasis on Australian soils. Soil Research 53, 605-635.

Nelson, M.A., Bishop, T.F.A., Triantafilis, J., Odeh, I.O.A., 2011. An error budget for different sources of error in digital soil mapping. European Journal of Soil Science 62, 417–430.

NSW Government, 2016. Climate Change Fund: Draft Strategic Plan 2017-2022. State of NSW and Office of Environment and Heritage, Sydney. https://www.environment.nsw.gov.au/-/media/OEH/Corporate-Site/Documents/Climate-change/draft-climate-change-fund-strategic-plan-160438.pdf (accessed 4 March 2019).

OEH, 2009. Protocols for soil condition and land capability monitoring. NSW Natural Resources Monitoring, Evaluation and Reporting Program. State of NSW and Department of Environment, Climate Change and Water NSW, Sydney. Available at http://www.environment.nsw.gov.au/resources/soils/SoilsProtocols.pdf [Accessed 4 March 2019].

OEH, 2014. Soil condition and land management in NSW: final results from the 2008–09 monitoring evaluation and reporting program. Technical Report. NSW Office of Environment and Heritage, Sydney, http://www.environment.nsw.gov.au/Research-and-publications/Publications-search/Soil-condition-and-land-management-in-New-South-Wales (accessed 4 March 2019).

OEH, 2017. NSW Landuse 2013, NSW Office of Environment and Heritage, Sydney. https://datasets.seed.nsw.gov.au/dataset/nsw-landuse-2013 [Accessed 4 March 2019].

OEH, 2018. Australian Soil Classification Soil Type Map of NSW. NSW Office of Environment and Heritage. https://espade.environment.nsw.gov.au (accessed 4 March.2019).

Orgill, S.E., Condon, J.R., Conyers, M.K., Morris, S.G., Murphy, B.W., Greene, R.S.B., 2017. Parent material and climate affect soil organic carbon fractions under pastures in south-eastern Australia. Soil Research, 2017, 55, 799–808.

Page, K.L., Dalal, R.C., Dang, Y., 2013. How useful are MIR predictions of total, particulate, humus, and resistant organic carbon for examining changes in soil carbon stocks in response to different crop management? A case study. Soil Research, 2013, 51, 719–725.

Poeplau, C., Don, A., Six, J., Kaiser, M., Benbi, D., Chenu, C., et al. 2018. Isolating organic carbon fractions with varying turnover rates in temperate agricultural soils – A comprehensive method comparison. Soil Biology & Biochemistry, 125, 10-26

R Core Team, 2018. 'The R Project for statistical computing'. R Foundation for Statistical Computing, Vienna, Austria. URL http://www.R-project.org/ (accessed 4 March.2019).

Rabbi, S.M.F., Tighe, M., Cowie, A., Wilson, B.R., Schwenke, G., McLeod, M., Badgery, W., Baldock, J., 2014. The relationships between land uses, soil management practices, and soil carbon fractions in South Eastern Australia. Agriculture, Ecosystems & Environment 197, 41–52. doi:10.1016/j.agee.2014.06.020

Rayment, G.E., Lyons, D.J., 2011. "Soil Chemical Methods – Australasia. Australian Soil and Land Survey Handbook Series, CSIRO Publishing, Melbourne.

Richards, G.P, Evans, D.M.W., 2004. Development of a carbon accounting model (FullCAM Vers. 1.0) for the Australian continent. Australian Forestry 67, No. 4, 277–283.

Robinson, N.J., Benke, K.K., Norng, S., 2015. Identification and interpretation of sources of uncertainty in soils change in a global systems-based modelling process. Soil Research 53:592-604.

Sanderman, J., Faquarson, R., Baldock, J., 2010. Soil Carbon Sequestration Potential: A review for Australian agriculture. CSIRO Land and Water, A report prepared for Department of Climate Change and Energy Efficiency, CSIRO, Canberra.

Sanderman, J., Baldock, J., Hawke, B., Macdonald, L., Massis-Puccini, A., Szarvas, S., 2011. 'National soil carbon research programme: field and laboratory methodologies.' CSIRO, Adelaide https://csiropedia.csiro.au/wp-content/uploads/2016/06/SAF-SCaRP-methods.pdf (accessed 4 March.2019).

Six, J., Guggenberger, G., Paustian, K., Haumaier, L., Elliott, E.T., Zech, W., 2001. Sources and composition of soil organic matter fractions between and within soil aggregates. European Journal of Soil Science 52, 607–618. doi:10.1046/j.1365-2389.2001.00406.x

Skjemstad, J.O., Spouncer, L.R., Cowie, B., Swift, R.S., 2004. Calibration of the Rothamsted organic carbon model (RothC ver. 26.3), using measurable soil organic pools. Australian Journal of Soil Research 42, 79–88. doi:10.1071/SR03013

Somarathna, P.D., Minasny, B., Malone, B.P., Stockmann, U., McBratney, AB 2018. Accounting for the measurement error of spectroscopically inferred soil carbon data for improved precision of spatial predictions. Science of the Total Environment 631-632, 377-389.

Stevenson, M., 2019. Package 'epiR': Tools for the Analysis of Epidemiological Data. CRAN Repository, https://cran.csiro.au/web/packages/epiR/epiR.pdf

Stockmann, U., Adams, M.A., Crawford, J.W., Field, D.J., Henakaarchchi, N., Jenkins, M., Minasny, B., McBratney, A.B., et al., 2013. The knowns, known unknowns and unknowns of sequestration of soil organic carbon. Agriculture, Ecosystems and Environment 164, 80– 99.

Vasques, G.M., Grunwald, S., Sickman, J.O., Comerford, N.B., 2010. Upscaling of dynamic soil organic carbon pools in a north-central Florida watershed. Soil Science Society of America Journal 74, 870–879.

Viscarra Rossel, R.A., 2011. Fine-resolution multiscale mapping of clay minerals in Australian soils measured with near infrared spectra. Journal of Geophysical Research 116, F04023, 15p

Viscarra Rossel, R.A., Lee, J., Behrens, T., Luo, Z., Baldock, J., Richards, A., 2019. Continental-scale soil carbon composition and vulnerability modulated by regional environmental controls. Nature Geoscience, https://doi.org/10.1038/s41561-019-0373-z

Viscarra Rossel, R.A., Webster, R., Bui, E.N., Baldock, J.A., 2014. Baseline map of organic carbon in Australian soil to support national carbon accounting and monitoring under climate change. Global Change Biology 20:2953-2970, doi: 10.1111/gcb.12569

van Wesemael, B., Chartin, C., Wiesmeier, M., von Lutzow, M., Hobley, E., et al., 2019. An indicator for organic matter dynamics in temperate agricultural soils. Agriculture, Ecosystems and Environment, 274, 62-75.

Vos, C., Jaconi, A, Jacobs, A., Don, A., 2018. Hot regions of labile and stable soil organic carbon in Germany. Soil, 4, 153-167.

Wiesmeier, M., Schad, P., von Lutzow, M., Poeplau, C., Spörlein, P., et al. 2014. Quantification of functional soil organic carbon pools for major soil units and land uses in southeast Germany (Bavaria). Agriculture, Ecosystems and Environment, 185, 208-220.

Wiesmeier, M., Urbanski, L., Hobley, E., Lang, B., von Lützow, M., et al. 2019. Soil organic carbon storage as a key function of soils - A review of drivers and indicators at various scales. Geoderma 333, 149–162.

Wilford, J., 2012. A weathering intensity index for the Australian continent using airborne gamma-ray spectrometry and digital terrain analysis. Geoderma 183, 124-142.

Wilson, B.R., King, D., Growns, I., Veeragathipillai, M., 2017. Climatically driven change in soil carbon across a basalt landscape is restricted to non-agricultural land use systems. Soil Research 55(4) 376-388 https://doi.org/10.1071/SR16205

Xiong, X., Grunwald, S., Myers, D.B., Kim, J., Harris, W.G., Comeford N.B., 2014. Holistic environmental soil-landscape modeling of soil organic carbon. Environmental Modelling & Software 57, 202–215.

Xu, M., Qi, Y., 2001. Spatial and seasonal variations of Q(10) determined by soil respiration measurements at a Sierra Nevadan forest. Global Biogeochemical Cycles 15, 687-696.

Yu, P., Han, K., Li, Q., Zhou, D., 2017. Soil organic carbon fractions are affected by different land uses in an agro-pastoral transitional zone in Northeastern China. Ecological Indicators 73, 331–337.

Zhang, H., Wu, P., Fan, M., Zheng, S., Wu, J., Yang, X., Zhang M., Yin, A., Gao, C., 2018. Dynamics and driving factors of the organic carbon fractions in agricultural land reclaimed from coastal wetlands in eastern China. Ecological Indicators 89, 639–647.

Zimmermann, M., Leifeld, J., Schmidt, M.W.I., Smith, P., Fuhrer, J., 2007. Measured soil organic matter fractions can be related to pools in the RothC model. European Journal of Soil Science 58, 658–667.

Supplementary Materials

Tables

Figures

Table S1. The average mean, standard deviation and standard error from the ten bootstrap predictions over the validation points[1]

Property	Depth (cm)	N	Mean	Standard deviation	Standard error
Total SOC stock	0-10	142	29.26	2.24	0.71
(Mg ha^{-1})	10-30	142	33.07	2.48	0.78
	0-30	142	63.37	4.30	1.36
POC stock	0-10	76	4.65	0.50	0.16
(Mg ha^{-1})	10-30	76	2.31	0.29	0.09
	0-30	75	7.41	0.73	0.23
HOC stock	0-10	76	13.55	1.02	0.32
(Mg ha^{-1})	10-30	76	17.74	1.57	0.50
	0-30	76	32.00	2.42	0.76
ROC stock	0-10	76	7.02	0.52	0.16
(Mg ha^{-1})	10-30	76	8.60	0.69	0.22
	0-30	76	15.99	1.06	0.33

[1] For each validation point, the mean, SD and SE were determined from the ten iterations. Then the mean of these values was calculated

Table S2. MLR model validation results

Property	Depth (cm)	N	LCCC	RMSE	Mean error
Total SOC stock	0-10	77	0.68	0.38	0.16
(log Mg ha^{-1})	10-30	77	0.58	0.35	0.16
	0-30	77	0.65	0.32	0.16
POC stock	0-10	77	0.74	0.50	0.24
(log Mg ha^{-1})	10-30	77	0.44	0.63	0.22
	0-30	77	0.62	0.48	0.24
HOC stock	0-10	77	0.66	0.34	0.14
(log Mg ha^{-1})	10-30	77	0.68	0.36	0.10
	0-30	77	0.70	0.31	0.12
ROC stock	0-10	77	0.64	0.33	0.14
(log Mg ha^{-1})	10-30	77	0.60	0.39	0.10
	0-30	77	0.63	0.32	0.12

Table S3. Standardised regression coefficients from MLR models

Soil forming factor	Variable	Total OC			POC			HOC			ROC		
		0-10	10-30	0-30	0-10	10-30	0-30	0-10	10-30	0-30	0-10	10-30	0-30
Climate													
	Rainfall	0.18	0.17	0.20	0.08	0.34	0.22	0.12	0.23	0.20	0.15	0.28	0.25
	Temp_max	-0.12	0.06	-0.04	-0.20	-0.02	-0.19	0.17	0.32	0.25	0.06	0.08	0.06
Parent material/soil													
	Lithology	-0.29	-0.50	-0.42	-0.14	-0.31	-0.21	-0.42	-0.58	-0.54	-0.37	-0.49	-0.47
	Kaolin prop'n	0.44	0.69	0.60	0.34	0.47	0.39	0.29	0.51	0.42	0.12	0.32	0.23
	Illite_prop'n	-0.05	-0.13	-0.10	-0.01	-0.11	-0.05	-0.05	-0.12	-0.09	-0.07	-0.15	-0.13
	Smectite_prop'n	0.07	0.23	0.15	0.16	0.42	0.29	-0.09	0.09	-0.003	-0.11	0.23	0.09
	Rad K	0.08	0.19	0.14	0.10	0.33	0.18	0.11	0.07	0.07	0.16	0.25	0.21
	Rad Th	-0.02	-0.05	-0.04	0.04	-0.22	-0.07	0.06	-0.01	0.02	-0.05	-0.21	-0.14
	Rad U	0.06	0.18	0.13	-0.04	-0.002	0.03	-0.02	0.05	0.05	-0.02	0.03	0.04
Relief													
	Aspect index	-0.05	0.001	-0.03	-0.01	-0.004	0.01	-0.12	-0.15	-0.14	-0.14	-0.10	-0.13
	Slope_pc	-0.07	0.004	-0.04	-0.14	-0.07	-0.12	-0.06	-0.06	-0.06	-0.07	-0.01	-0.03
	Topo slope index	-0.03	-0.02	-0.02	-0.04	-0.03	-0.05	-0.07	-0.08	-0.08	-0.01	0.10	0.05
	Topo wet index	-0.02	0.001	-0.01	-0.06	-0.04	-0.07	-0.05	-0.06	-0.06	-0.09	-0.04	-0.07
Biota													
	Land_disturb_ index	-0.17	-0.07	-0.13	-0.28	-0.15	-0.28	-0.10	0.03	-0.03	-0.17	-0.10	-0.14
	Veg frac cover	0.31	0.03	0.18	0.35	-0.22	0.08	0.50	0.21	0.35	0.44	0.05	0.22
Age													
	Weathering index	0.07	0.26	0.18	-0.01	0.10	0.04	0.08	0.06	0.07	0.03	0.04	0.03

Figure S1. SOC carbon fraction masses over NSW, mean and upper and lower 95% prediction intervals, 0-10 cm (kg m^{-3})

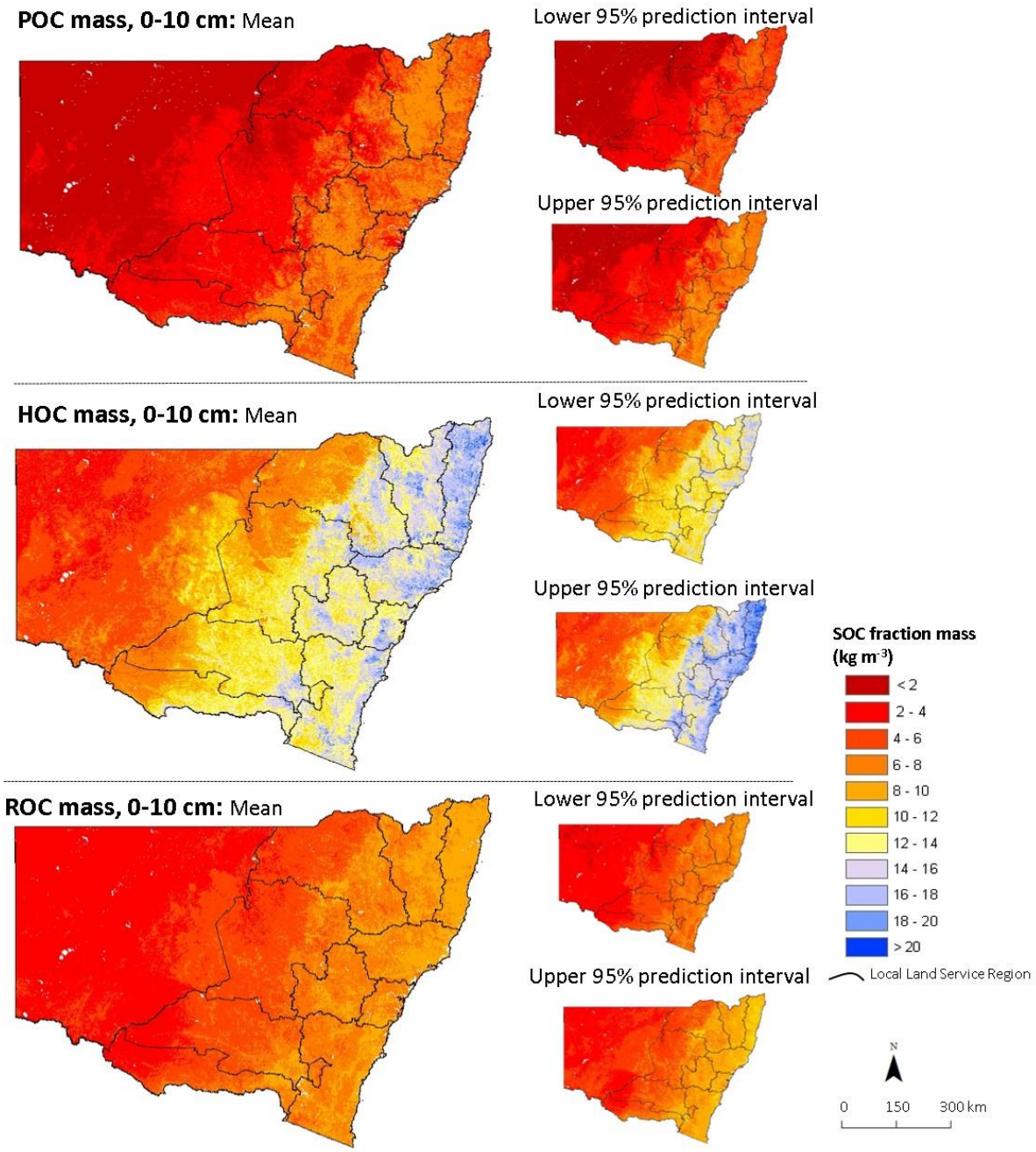

Note: these maps presented as SOC mass (kg m^{-3}) rather than stocks (Mg ha-1) to facilitate more meaningful comparison of the upper (0-10 cm) and lower (10-30 cm) layers. Conversion to stocks is achieved by multiplying the upper layer by 1 (ie, unchanged) and the lower layer by 2.

Figure S2. SOC carbon fraction masses over NSW, mean and upper and lower 95% prediction intervals, 10-30 cm (kg m^{-3})

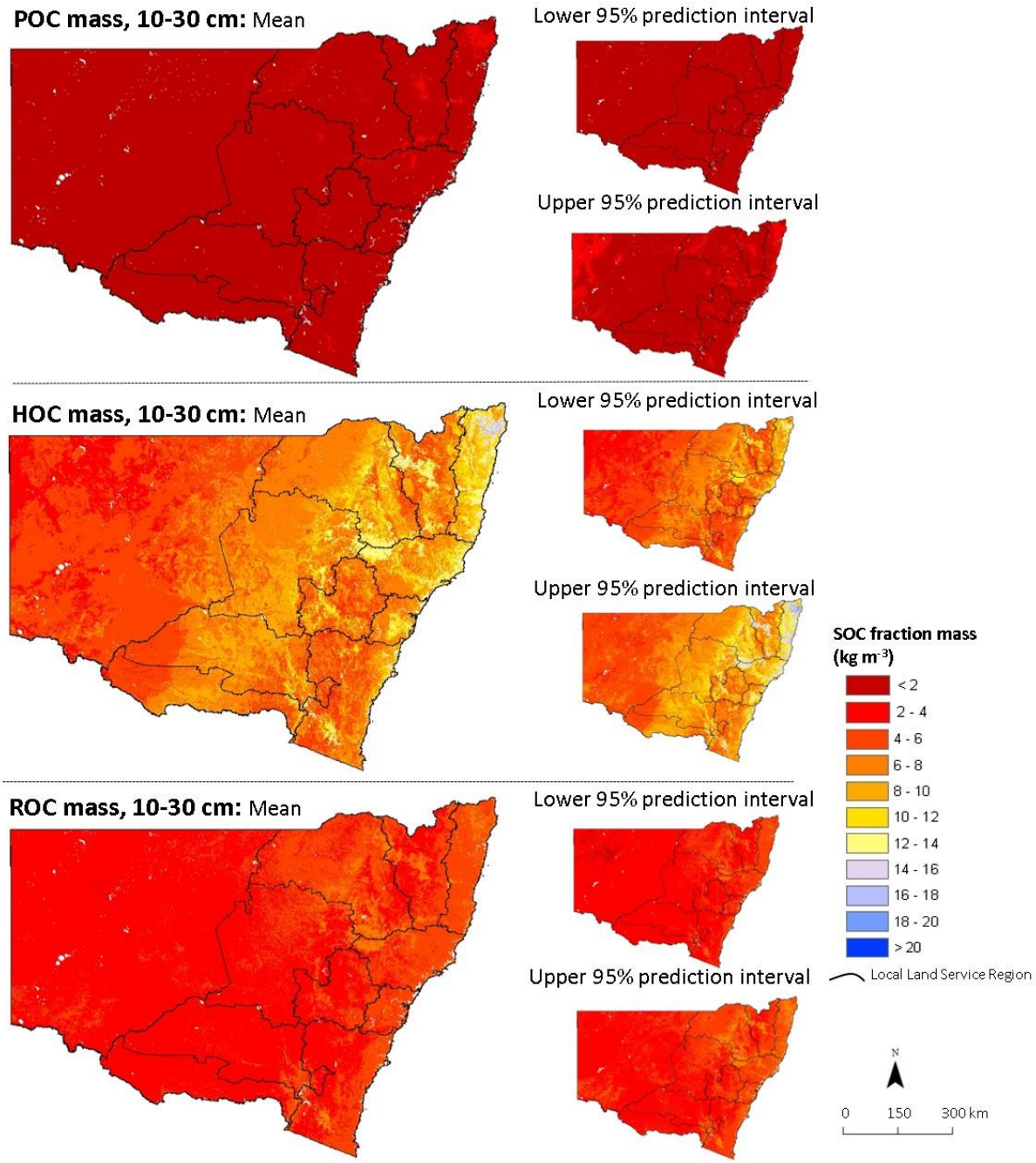

Figure S3. Variable importance plots for absolute stocks of the three carbon fractions, 0-10 and 10-30 cm (+ or – sign gives direction of influence, from Table S2)